

PHILOSOPHICAL TRANSACTIONS OF THE ROYAL SOCIETY A

MATHEMATICAL, PHYSICAL AND ENGINEERING SCIENCES

Solid solution formation in the metatorbernite- metazeunerite system ($\text{Cu}(\text{UO}_2)_2(\text{PO}_4)_{2-x}(\text{AsO}_4)_x \cdot n\text{H}_2\text{O}$) and their stability under conditions of variable temperature.

Journal:	<i>Philosophical Transactions A</i>
Manuscript ID	RSTA-2018-0242.R1
Article Type:	Research
Date Submitted by the Author:	n/a
Complete List of Authors:	Kirk, Caroline; University of Edinburgh, Chemistry; University of Edinburgh, Centre for Science at Extreme Conditions; The Natural History Museum, Earth Sciences Kulaszewska, Joanna; Loughborough University, Chemistry Dann, Sandra; Loughborough University, Chemistry Warwick, Peter; Loughborough University, Chemistry
Issue Code (this should have already been entered but please contact the Editorial Office if it is not present):	SYNCHOTRON
Subject:	Environmental Chemistry (67) < CHEMISTRY (1002), Materials Science (117) < CHEMISTRY (1002), Crystallography (56) < CHEMISTRY (1002)
Keywords:	Metatorbernite, Metazeunerite, solid-solution, diffraction, variable temperature

SCHOLARONE™
Manuscripts

1
2
3
4
5
6
7
8
9
10
11
12
13
14
15
16
17
18
19
20
21
22

Solid solution formation in the metatorbernite- metazeunerite system ($\text{Cu}(\text{UO}_2)_2(\text{PO}_4)_{2-x}(\text{AsO}_4)_x \cdot n\text{H}_2\text{O}$) and their stability under conditions of variable temperature.

23
24
25
26
27

Joanna Kulaszewska¹, Sandra Dann¹, Peter Warwick¹ and
Caroline Kirk^{*2,3,4}

28
29

1. Department of Chemistry, Loughborough University, Loughborough, LE11 3TU, U.K.

2. School of Chemistry, University of Edinburgh, Edinburgh, EH9 3FJ, U.K.

30
31

3. Centre for Science at Extreme Conditions, University of Edinburgh, Edinburgh, EH9 3FD, U.K.

32
33

4. Department of Earth Sciences, The Natural History Museum, London, SW7 5BD, U.K.

34
35

Keywords: Metatorbernite, metazeunerite, solid-solution, diffraction, synchrotron, variable-temperature

36
37
38

Summary

39
40
41
42
43
44
45
46
47
48
49
50
51
52
53
54
55
56
57
58
59
60

Mineral phases which can be thought of as members of a metatorbernite -metazeunerite solid solution ($\text{Cu}(\text{UO}_2)_2(\text{PO}_4)_{2-x}(\text{AsO}_4)_x \cdot 8\text{H}_2\text{O}$) have been identified in radioactive samples from spoil heaps at the uranium mine site in South Terras, Cornwall (grid reference SW935523). A complete solid solution ($0 < x < 2$) was synthesised by precipitation from solution using uranium (VI) nitrate and copper (II) chloride and phosphoric acid/arsenic acid in the appropriate molar proportions. Refined unit cell parameters determined by Pawley fitting of powder X ray Diffraction data, showed a linear variation in the a unit cell parameter according to Vegard's Law, allowing the composition of the natural mineral phases found at South Terras to be determined from measurement of their unit cell parameters. High resolution variable temperature synchrotron powder X ray diffraction studies were carried out at the Diamond Light Source on three members of this solid solution ($x = 0, 1, 2$) and showed different structural behaviour as a function of composition and temperature. Metatorbernite ($x=0$) retains its tetragonal symmetry at low temperatures and dehydrates to an amorphous phase at 473K, whereas metazeunerite ($x=2$) transforms to an orthorhombic phase at low temperatures, regains its tetragonal symmetry on heating to 323K and undergoes a further transition to an, as yet, unidentified phase at 473K.

*Author for correspondence (Caroline.Kirk@ed.ac.uk).

Present address: School of Chemistry, University of Edinburgh,
Edinburgh, EH9 3FJ, U.K

1 *R. Soc. open sci.* article template

2 2 Metatorbernite-metazeunerite solid solution

13 Introduction

14
15 Metatorbernite ($\text{Cu}(\text{UO}_2)_2(\text{PO}_4)_2 \cdot 8\text{H}_2\text{O}$), is a common secondary mineral resulting from pitchblende (UO_2)
16 alteration and can be considered as a significant host for uranium in both natural and anthropogenically
17 contaminated environments [1]. Uranyl phosphates, such as metatorbernite, are known for their low solubility
18 at circumneutral pH and are considered important for the control of uranium mobility in the environment
19 under oxidising conditions [2]. It has been suggested that U-contaminated groundwater may be
20 decontaminated through the application of polyphosphates to form sparingly soluble uranyl phosphate
21 phases, such as metatorbernite [3].
22
23
24
25
26
27
28

29 The disused uranium mine in South Terras, Cornwall, has been abandoned for nearly a century, but discarded
30 spoil heaps at the site still retain significant levels of activity [4]. The interest in this site is part of a larger
31 study into the fate of radionuclides in the environment (NERC Long-lived Radionuclides In the Surface
32 Environment (Lo-RISE) project). While previous studies have indicated that uranium in these spoil heaps is
33 relatively immobile [5, 6], there are no published studies reporting the exact composition and stability of the
34 uranium solid-state phases present in the spoil heaps. Metatorbernite has been reported to be present in areas
35 of this locality [4, 5], along with the arsenate analogue of this mineral phase, metazeunerite
36 ($\text{Cu}(\text{UO}_2)_2(\text{AsO}_4)_2 \cdot 8\text{H}_2\text{O}$). A 2017 study indicated the possibility of a phosphate containing metazeunerite
37 phase existing at this locality [7].
38
39
40
41
42
43
44
45

46 Metatorbernite is a member of the autunite family of minerals, which are some of the most widespread and
47 abundant secondary uranium minerals known [8]. The composition of this family of minerals is variable with
48 the ideal formula $\text{A}(\text{UO}_2)_2(\text{XO}_4)_2 \cdot n\text{H}_2\text{O}$, where A is a divalent cation, X is arsenic or phosphorus and n is in the
49 region of 10-16 for the autunite group and 6-8 for the meta-autunite group [9]. The mineral autunite has the
50 ideal composition $\text{Ca}(\text{UO}_2)_2(\text{XO}_4)_2 \cdot 10\text{-}12\text{H}_2\text{O}$ and is less stable than the phase meta-autunite,
51 $\text{Ca}(\text{UO}_2)_2(\text{PO}_4)_2 \cdot 8\text{H}_2\text{O}$ [10]. There are other known mineral phases related to autunite with monovalent or,
52
53
54
55
56
57

58 *Phil. Trans. R. Soc. A.*

1
2
3
4
5
6
7
8
9 more rarely, trivalent cations. The ideal formula for these phases is slightly altered to $M^+(UO_2)(XO_4).nH_2O$ or
10 $M^{3+}(UO_2)(XO_4).nH_2O$ [9, 11].
11
12

13
14 The structures of autunite and meta-autunite minerals are mostly reported to crystallise in primitive
15 tetragonal space groups. However, there are also reports of phases crystallising in orthorhombic, monoclinic
16 and triclinic space groups as well [11]. The structure can be described as sheets of uranyl arsenate/phosphate,
17 with the composition $[(UO_2)_2(XO_4)_2]^{2-}$, $X = P$ or As , stacked along the c axis with the cations and varying
18 numbers of water molecules situated between the sheets (figure 1) [12, 13].
19
20
21
22

23
24 The published structural models for metatorbernite and metazeunerite are all primitive tetragonal, however,
25 there are inconsistencies in the reported unit cell parameters and a number of different space groups have been
26 used to describe their structures. Previous structural studies on metatorbernite and metazeunerite phases have
27 been carried out on mineral samples using X ray diffraction techniques [12, 14-21]. The work presented in this
28 paper focuses on refinement of unit cell parameters of synthetic phases only and further work on full
29 structural characterisation is underway [22].
30
31
32
33
34

35
36 In this paper we report the synthesis and characterisation of a metatorbernite-metazeunerite $(Cu(UO_2)_2(PO_4)_{2-x}(AsO_4)_x.8H_2O)$
37 solid solution for $0 < x < 2$. Powder X ray Diffraction (PXRD) data collected on these synthetic
38 samples are compared with PXRD data collected on spoil heap samples removed from the disused uranium
39 mine in South Terras, Cornwall to determine the composition of the naturally occurring mineral
40 metatorbernite-type phases identified. Variable temperature studies carried out on the high resolution powder
41 diffraction beamline I11 at the Diamond Light Source [23] on three solid solution compositions,
42 $Cu(UO_2)_2(PO_4)_{2-x}(AsO_4)_x.8H_2O$ ($x = 0, 1, 2$) are also reported and show different behaviour according to the
43 value of x .
44
45
46
47
48
49
50
51
52
53
54
55
56
57

1 *R. Soc. open sci.* article template

2 4 Metatorbernite-metazeunerite solid solution

10 Methods

13 (a) Sampling

16 Sampling of the South Terras site was carried out in July 2015. Two sites of interest were identified using a
17 handheld LB124 Berthold monitor; these were named Mine Spoil (MS) and Ore Processing Floor (OPF). About
18 10 litres of soil and/or spoil were removed from the surface of each site using a hand shovel to a depth of
19 about 20-30 cm. The samples were packed and stored in clean, polypropylene boxes before being transported
20 to Loughborough University. All samples were dried in an oven at 80 °C before being gently crushed with a
21 pestle and mortar. They were then placed into a laboratory sieve shaker and separated into size fractions: > 2
22 mm and < 2 mm. The > 2 mm fraction from the MS sample was spread out in a tray and monitored using a
23 Geiger-Müller counter. Individual samples of especially high activity (≥ 100 cps) were separated and labelled
24 as high activity (HA) samples for further analysis.

33 (b) Synthesis

36 Metatorbernite was synthesised by adapting a method described by Cretaz [2]. 2.5g Uranyl nitrate
37 hexahydrate (Aldrich) was dissolved in 25 mL of a 0.5×10^{-2} mol L⁻¹ solution of nitric acid. 0.44 g copper (II)
38 chloride dihydrate (reagent grade Sigma Aldrich) was added and shaken until dissolved. 2.5 mL of a 2 M
39 solution of phosphoric acid (reagent grade Sigma Aldrich) was then added. After approximately one hour,
40 pale green crystals were observed to form. The crystals were left on a shaker at room temperature for 1 h
41 before being left to settle for 48 h. The product was then filtered under vacuum using a 0.1 µm cellulose
42 membrane and washed three times with deionised water. The crystals were left to dry in an oven at 40°C until
43 a constant weight was achieved.

46 Metazeunerite was prepared using the same method but replacing the phosphoric acid with a 2 M solution of
47 arsenic acid. The arsenic acid was prepared by dissolving 2.5 g arsenic (V) oxide (sigma Aldrich reagent
48 grade) in 10 mL of deionised water.

58 *Phil. Trans. R. Soc. A.*

Members of the solid solution were prepared using different ratios of phosphoric and arsenic acid in the synthetic mixture to produce the compositions $\text{Cu}(\text{UO}_2)_2(\text{PO}_4)_{2-x}(\text{AsO}_4)_x \cdot n\text{H}_2\text{O}$, $x = 0.2, 0.4, 0.5, 0.6, 0.8, 1.0, 1.2, 1.4, 1.5, 1.6$ and 1.8 .

(c) Powder X Ray Diffraction

Powder X-ray diffraction data were collected using a Bruker D8 Discover X-ray diffractometer in transmission geometry using $\text{Co K}\alpha_1$ radiation, selected using a Ge 111 single crystal monochromator and a Braun Position Sensitive detector. For phase identification of samples, data were collected over the 2θ range $5-60^\circ$ with a step size of $0.0072334^\circ 2\theta$ and a count time of 0.5s per step. For refinement of structural parameters, data were collected over the 2θ range $9-80^\circ$ with a step size of $0.0072334^\circ 2\theta$ and a count time of 5.2s per step.

Synchrotron powder diffraction data were collected using a Si-calibrated wavelength of $\lambda = 0.82603 \text{ \AA}$ on the high-resolution powder X-ray diffraction beamline I11 at the Diamond Light Source, UK [23]. The samples were packed into 0.5 mm borosilicate capillary tubes and secured with Kapton tape. Data were collected in transmission geometry using multi-analysing crystal detectors over an angular range of $1 - 150^\circ 2\theta$. The PXRD data were collected at 293 K for 30 minutes. Samples were then cooled using the Cryostream Plus to 105-110 K and a new dataset was collected for 30 minutes. Data were collected on heating at 50K intervals until a temperature of 500K was reached.

For the purposes of phase identification, the PXRD data patterns were compared to known end-member phases in the International Centre for Diffraction Data (ICDD) Powder Diffraction File (PDF2) database using the search match software contained in the software suite WinXPow. For the refinement of structural parameters, data were analysed using the software Topas Academic V6 [24].

(d) ICP-OES

0.2 g of either the solid solution phase or mineral sample was weighed into a 15 mL polypropylene centrifuge tube. It was then dissolved in 2 mL 50% HNO_3 . A 0.1 mL aliquot of sample was removed and added to a 15 mL centrifuge tube, this was then diluted to 10 mL using more 2% HNO_3 in deionised water. Elemental analysis was carried out using a Thermo Scientific 6000 series ICAP-6500 duo ICP-OES .

Phil. Trans. R. Soc. A.

1 R. Soc. open sci. article template

2 6 Metatorbernite-metazeunerite solid solution

11 Results and Discussion

14 PXRD data collected on the samples from South Terras which were shown to have high activity (≥ 100 cps),
15 identified the presence of metatorbernite-type phases. Figure 2 shows an example of one of the datasets
16 collected on sample HR 001, which was found to contain quartz as an impurity phase. The powder diffraction
17 data did not match exactly with any of the metatorbernite diffraction patterns contained in the database
18 (ICDD PDF2) as the observed peak positions were found to be shifted relative to the database patterns. We
19 confirmed this was a sample effect and not due to misalignment of the diffractometer or the sample
20 preparation method by adding a silicon internal standard (not shown in this dataset). We propose that the
21 composition of the sample deviates from that of metatorbernite and could be a member of a solid solution
22 between metatorbernite and metazeunerite as the observed peak positions were found to lie between the
23 reflection positions of metatorbernite, (ICDD PDF 36-406 [15]) and metazeunerite (ICDD PDF 17-146 [25]).
24 ICP-OES analysis confirmed the presence of As in these samples. The results from the sample HR 001 are
25 presented in supplementary figure 1 and show the presence of Cu, U, As and P, which can be related to an As-
26 containing metatorbernite-type phase. Fe, Al, Pb and Si are observed in small quantities due to the presence of
27 impurity phases, present in quantities below the detection limits of PXRD techniques. There are only a few
28 reports in the literature regarding the cross-substitution of phosphorus and arsenic in the metatorbernite-type
29 system in nature [3]. Corkhill *et al* reported a phosphate containing metazeunerite phase at South Terras,
30 present as a thin crust on minerals such as muscovite and jarosite. [7]. The only report of similar solid solution
31 behaviour is in the related system $\text{H}(\text{UO}_2)(\text{PO}_4)_{1-x}(\text{AsO}_4)_x \cdot 3\text{H}_2\text{O}$ [26, 27].
32
33
34
35
36
37
38
39
40
41
42
43
44
45

46 To confirm the hypothesis that a solid solution between metatorbernite and metazeunerite exists, a synthetic
47 study was carried out. We prepared compositions of the proposed solid solution $\text{Cu}(\text{UO}_2)_2(\text{PO}_4)_{2-x}(\text{AsO}_4)_x \cdot n\text{H}_2\text{O}$,
48 $0 < x < 2$, in 0.2 increments. PXRD data were collected on the samples and found that a
49 complete solid solution existed with no evidence for the presence of any impurity phases. Synchrotron PXRD
50 data collected on selected samples of the solid solution are presented in supplementary information figure 2.
51
52
53
54
55
56
57

58 *Phil. Trans. R. Soc. A.*

Pawley refinements of the lab PXRD data in space group $P4/n$ were carried out and the refined unit cell parameters as a function of composition, x , are presented in figure 3. The refined unit cell parameters are $a = 6.9736$ (9) Å and $c = 17.341$ (2) Å for metatorbernite and $a = 7.1204$ (9) Å and $c = 17.442$ (3) Å for metazeunerite. Comparison with the reported unit parameters for the end member phases by Locock *et al.*, of $a = 6.98$ (5) Å and $c = 17.35$ (2) Å for metatorbernite and $a = 7.11$ (1) Å and $c = 17.42$ (1) Å for metazeunerite show our findings are consistent with previous studies [12]. It should be noted that the reported unit cell parameters for both metatorbernite and metazeunerite show some variation, with a wider range found for reported c parameters. For metatorbernite, a was found to range between 6.95 Å [19] and 6.98 Å [17, 12] and c between 17.28 Å [20] and 17.41 Å [17], whereas for metazeunerite the range of refined a unit cell parameters was between 7.10 Å [17] and 7.13 Å [14] and a wider range for c of between 17.38 Å [17] and 17.70 Å [16].

The variation in reported values could be due to compositional variations away from the ideal (i.e. $\text{Cu}(\text{UO}_2)_2(\text{XO}_4)_2 \cdot 8\text{H}_2\text{O}$, $X = \text{P}$ or As) as all studies were carried out on mineral samples and there is a possibility that the X site is not pure P or As, and/or Cu may have been replaced with other metal cations (e.g. Ca, Fe) as well as the water content not being exactly 8 molecules per formula unit. [12, 14 – 21]. The refined unit cell parameters of the solid solution members show a (nearly) linear trend as a function of composition, which is more obvious in terms of the a parameter than the c parameter. Due to the layered nature of the structure (figure 1), a change in the number water molecules per formula unit between the layers would have more impact on c than a . All the synthetic samples were dried at 40 °C to ensure the transformation from torbernite-type to metatorbernite-type phases was complete. The torbernite-type samples are more hydrous, with a reported twelve water molecules per formula unit and are less stable than the metatorbernite-type samples (with eight water molecules per formula unit), on which this study focuses. It was found that the compositions containing more arsenate ions required longer times to fully complete the transformation. Further investigations are underway to establish what variability exists in terms of water content.

Using the linear correlation between the a parameter and the AsO_4/PO_4 ratio (equation 1, figure 3), the formulae of two natural samples taken from South Terras were determined (Table 1). A comparison of the observed data collected on the natural samples to the observed data on the solid solution member with the same approximate composition, showed good agreement. (Supplementary information figures 3 and 4)

Phil. Trans. R. Soc. A.

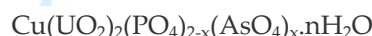
1 R. Soc. open sci. article template

2 8 Metatorbernite-metazeunerite solid solution

3
4
5
6
7
8
9
10
11
12 Our results show that the abundance of arsenic on the South Terras site is significant and natural samples
13 contain mixtures of the two species where arsenate is significant and possibly dominant. While the stability of
14 the phosphate end member in the natural environment has been documented [2], much less is known about
15 the arsenate material or samples with a mixed composition of the AsO_4/PO_4 species, which appear to be
16 present naturally. This suggests stability studies on the mixed anion materials will be of major interest in
17 assessing the stability of the mine spoil on a long term basis.
18
19
20
21
22

$$y = 0.0778x + 6.9707$$

23
24
25 **Equation 1:** Relationship between refined a parameter and composition in terms of x for the solid solution



26
27
28
29
30 The scatter in the refined unit cell c parameter between metatorbernite and metazeunerite could be due to
31 several reasons, variation in the water content, as highlighted above or differences in the space group between
32 the two systems. We have carried out preliminary structural refinements of the high resolution synchrotron
33 data collected on metatorbernite, which refined well in space group $P4/n$ and metazeunerite, with data fitting
34 better in space group $P4/ncc$ [22]. However, there are real difficulties with refining these structures by X-ray
35 diffraction due to the dominant scattering of uranium compared to all other species, anion disorder and the
36 complexity of this structure. Powder neutron diffraction data will be required to resolve these issues.
37
38
39
40
41
42
43

44 Variable temperature studies on three solid solution compositions, $\text{Cu}(\text{UO}_2)_2(\text{PO}_4)_{2-x}(\text{AsO}_4)_x \cdot 8\text{H}_2\text{O}$ ($x = 0, 1, 2$)
45 over the temperature range 110K-500K were also carried out. There was noticeable variability in the behaviour
46 of different compositions as a function of temperature. The metatorbernite sample remained tetragonal on
47 cooling and decomposed on heating, showing an amorphous signature at temperatures $> 473\text{K}$, which
48 recrystallized on cooling to produce an as yet unidentified phase. The high resolution synchrotron powder
49 diffraction data are presented in supplementary figure 5 and the refined unit cell parameters plotted as a
50 function of temperature are shown in figure 4. The unit cell parameters were refined in space group $P4/n$ over
51
52
53
54
55
56
57

58 *Phil. Trans. R. Soc. A.*

1
2
3
4
5
6
7
8
9 the temperature range 105 – 443K. Both unit cell parameters were found to expand linearly, with c expanding
10 more than a . A plot of a/c versus temperature (supplementary figure 6) shows the linear expansion up to 373K
11 and then a deviation from linearity, which could indicate the beginnings of a dehydration process.
12
13

14
15 The composition $\text{Cu}(\text{UO}_2)_2(\text{PO}_4)(\text{AsO}_4) \cdot 8\text{H}_2\text{O}$ was studied over the temperature range 110 – 473K and its
16 behaviour was found to be different to that of the end member phases. The sample remains tetragonal on
17 cooling, as in the case of metatorbernite but on heating to 423K, the diffraction pattern shifts to higher 2 theta
18 values and can be indexed in space group P4/n, with smaller unit parameters refined as $a = 7.08224(4) \text{ \AA}$ and c
19 $= 16.7862(2) \text{ \AA}$ (figure 4). On further heating to 473K, the diffraction pattern changes completely forming a
20 new structure that is still to be identified. The variable temperature data collected on this composition are
21 given in supplementary information (supplementary figure 7) and a plot of the a/c ratio as a function of
22 temperature (supplementary figure 8). As with the metatorbernite phase, a linear expansion with temperature
23 is observed up to 323K and the trend is found to be non-linear above these temperatures, which could indicate
24 the start of the dehydration process.
25
26
27
28
29
30
31
32
33

34 Figure 4 presents the refined unit cell parameters from the high temperature PXRD studies of metatorbernite
35 and the composition $\text{Cu}(\text{UO}_2)_2(\text{PO}_4)(\text{AsO}_4) \cdot 8\text{H}_2\text{O}$ compared to published unit cell parameters from a high
36 temperature PXRD study carried out on a mineral sample [28]. The composition of this mineral sample was
37 determined to be $\text{Cu}(\text{UO}_2)_2(\text{PO}_4)_{1.9}(\text{AsO}_4)_{0.1} \cdot 2\text{H}_2\text{O}$ by EPMA. Their findings show that at 129 °C (402K), the
38 diffraction pattern can be indexed in space group P4/n with a smaller unit cell ($a = 6.9551(3) \text{ \AA}$, $c = 16.6604(9)$
39 \AA) than the parent metatorbernite phase. This trend is similar to our results, whereby the mixed
40 arsenate/phosphate composition shows a decrease in a and c unit cell parameters at 423K. We suggest the
41 deviation between the two studies are due to the different compositions of the phases analysed.
42
43
44
45
46
47
48

49 The metazeunerite sample was studied over the temperature range 110 – 473K and exhibits different
50 behaviour on heating and cooling, whereby on cooling the symmetry of the sample is lowered and the
51 diffraction pattern can be indexed on an orthorhombic unit cell with proposed space group Pccn, $a = 7.1138(2)$
52 \AA , $b = 7.1584(3) \text{ \AA}$, $c = 17.5439(9) \text{ \AA}$. On heating back to room temperature, the structure remains
53 orthorhombic until 323K, with the room temperature dataset refined as a mixture of tetragonal and
54
55
56
57

58 *Phil. Trans. R. Soc. A.*
59
60

1 *R. Soc. open sci.* article template

2 10 Metatorbernite-metazeunerite solid solution

3
4
5
6
7
8
9
10 orthorhombic phases. It may be that a more controlled heating rate would allow the sample to transform to
11 the tetragonal phase at room temperature and this needs further investigation. The sample remains tetragonal
12 until 373 K and above this temperature forms a new phase, with an unknown structure. The variable
13 temperature data collected on metazeunerite are presented in supplementary figure 9 and figure 5 shows a
14 plot of the refined lattice parameters as a function of temperature. The reversible tetragonal to orthorhombic
15 phase transition is clearly shown on the refined unit cell parameter versus temperature plot (figure 5). Over
16 the temperature range 110 – 373 K, a linear expansion in the unit cell volume is observed.

17
18
19
20
21
22
23
24 The phase changes that occur in metatorbernite and metazeunerite at high temperature have been studied
25 previously using X ray diffraction, thermogravimetric analysis and Raman spectroscopy [28-33]. Most of the
26 studies have been carried out on mineral samples and there is a lack of consistency in the findings due to the
27 compositional variation in the samples.

28
29
30
31
32 Suzuki *et al* carried out HTXRD and TGA on a mineral sample of metatorbernite and reported a weight loss at
33 86°C that equated to 4 or 5 molecules of H₂O per formula unit [29]. The XRD pattern collected at 100°C
34 showed a shift in two theta positions when compared to the dataset collected at room temperature, with the
35 basal spacing decreasing from 8.61Å to 8.07Å. The authors claim that the dehydrated phase at this
36 temperature is likely to have the composition Cu(UO₂)₂(PO₄)₂.4H₂O, losing water molecules from between the
37 uranyl phosphate sheets, but retaining the layered structure. On further heating the sample showed another
38 weight loss and change in diffraction pattern at ~200°C and Suzuki and co-workers stated that the dehydrated
39 phase at this temperature has the likely composition Cu(UO₂)₂(PO₄)₂.2H₂O, with a basal spacing of 6.58 Å. On
40 heating further to 300 °C, there are two reflections with *d* spacings of 6.52 and 5.60 Å; the authors interpret the
41 appearance of the these reflections as being due to the presence of two different hydration states with likely
42 compositions Cu(UO₂)₂(PO₄)₂.H₂O and anhydrous Cu(UO₂)₂(PO₄)₂. There is no evidence from their HT PXRD
43 study of any amorphous phase forming under these conditions, as we observed with the synthetic
44 metatorbernite phase at temperatures greater than 423K. It should be noted, that they only reported the *d*
45 spacings of the basal spacing of the phases formed on heating with no refined unit cell parameters given.

46
47
48
49
50
51
52
53
54
55
56
57
58 *Phil. Trans. R. Soc. A.*

1
2
3
4
5
6
7
8
9 Suzuki *et al* compare their findings with that of Vochten *et al* [30], who carried out TGA studies on
10 metatorbernite and found weight loss steps at 120 °C, 150 °C and 150-400 °C, which they stated were the
11 temperatures where the compositions $\text{Cu}(\text{UO}_2)_2(\text{PO}_4)_2 \cdot 4\text{H}_2\text{O}$, $\text{Cu}(\text{UO}_2)_2(\text{PO}_4)_2 \cdot 2\text{H}_2\text{O}$ and $\text{Cu}(\text{UO}_2)_2(\text{PO}_4)_2$
12 formed.

13
14
15 Stubbs *et al* [28] studied a mineral sample, that was shown to have the composition
16 $\text{Cu}(\text{UO}_2)_2(\text{PO}_4)_{1.9}(\text{AsO}_4)_{0.1} \cdot 2\text{H}_2\text{O}$ by EPMA, using HT XRD over the temperature range RT to 315 °C. These
17 authors carried out more in depth structural analysis on the phases formed on dehydration than Suzuki and
18 reported preliminary structural models for two of the dehydrated phases. Their findings state that at 129 °C, a
19 phase crystallising in the space group P4/n with a smaller unit cell than the parent metatorbernite phase was
20 formed with a suggested formula of $\text{Cu}(\text{UO}_2)_2(\text{PO}_4)_2 \cdot 6\text{H}_2\text{O}$, on further heating to 173 °C, the sample
21 dehydrates to $\text{Cu}(\text{UO}_2)_2(\text{PO}_4)_2 \cdot 3\text{H}_2\text{O}$ and recrystallises in space group P21. There is a further phase which
22 formed at higher temperatures (209-315 °C), but at the maximum temperature used in this study there was
23 still evidence for the presence of the phase $\text{Cu}(\text{UO}_2)_2(\text{PO}_4)_2 \cdot 3\text{H}_2\text{O}$; no structural model or suggested
24 composition was given for this phase. Stubbs *et al* compared their work to that of Frost *et al* [31], who carried
25 out controlled rate thermal analysis on a mineral sample of metatorbernite, whereby the heating rate was
26 varied according to whether the sample was undergoing a dehydration event or not. Frost found three mass
27 losses which they equated to the compositions $\text{Cu}(\text{UO}_2)_2(\text{PO}_4)_2 \cdot 6.5\text{H}_2\text{O}$ (at 138 °C), $\text{Cu}(\text{UO}_2)_2(\text{PO}_4)_2 \cdot 2\text{H}_2\text{O}$ (at
28 155°C) and $\text{Cu}(\text{UO}_2)_2(\text{PO}_4)_2$ (at 291°C).

29
30
31
32
33
34
35
36
37
38
39
40
41 Our PXRD study on the synthetic analogue of the pure metatorbernite composition at elevated temperatures,
42 does not follow the dehydration profile of either of the reported HT XRD studies on mineral samples of
43 metatorbernite [28, 29]. We suggest that the differences are due to several factors. Firstly the sample
44 environment is different, in this study the sample is in a sealed capillary and therefore its dehydration
45 behaviour is different to that of a sample which is heated in an open system. Secondly, the compositional
46 variations are key. This synthetic sample is a pure copper uranyl phosphate, whereas the mineral samples
47 were shown to be either two phase by PXRD [29] or contain arsenate as well as phosphate through EPMA [28].
48 As discussed above, the dehydration behaviour of the mixed phosphate arsenate composition
49 ($\text{Cu}(\text{UO}_2)_2(\text{AsO}_4)_2 \cdot 8\text{H}_2\text{O}$) is more in line with that of Stubbs [28], see figure 5.
50
51
52
53
54
55
56
57

58 *Phil. Trans. R. Soc. A.*
59
60

R. Soc. open sci. article template

12 Metatorbernite-metazeunerite solid solution

Two studies of the high temperature behaviour of metazeunerite have been reported [32, 33], both studies analyse metazeunerite samples using TGA techniques, but neither carry out any *in situ* HTXRD studies. The study by Frost is on a mineral sample that is stated to be a mixture of zeunerite and metazeunerite, as determined by PXRD analysis. The results of the TGA study, which were carried out under a N₂ atmosphere, are discussed in terms of the sample being single phase metazeunerite and are linked to a HT Raman study carried out on the same sample. Frost *et al* [32] show three weight losses that are claimed to be the loss of water, which would give the following compositions on heating Cu(UO₂)₂(AsO₄)₂·6H₂O (48 °C), Cu(UO₂)₂(AsO₄)₂·2H₂O (88 °C) and Cu(UO₂)₂(AsO₄)₂ (125-250 °C).

Vochten *et al* [33] carried out a TGA study, under a flow of air, on a synthetic sample of metazeunerite, prepared under different conditions to the synthetic samples in our study. They showed four stages of dehydration which would give the following compositions on heating, Cu(UO₂)₂(AsO₄)₂·7H₂O (108 °C), Cu(UO₂)₂(AsO₄)₂·3H₂O (130 °C), Cu(UO₂)₂(AsO₄)₂·2.5H₂O (185 °C) and Cu(UO₂)₂(AsO₄)₂ (230 °C). Our study did not use a flow of gas, the samples were sealed in borosilicate capillaries and therefore the dehydration behaviour is shown to be different, with only one change in structure observed at 150 °C, to an as yet unidentified phase.

All these studies highlight the variability in the behaviour of metatorbernite-type phases as a function of temperature. The heating rate and atmosphere will play a role in how these phases dehydrate, but the composition is key too, with differences between mineral and synthetic samples shown as well as differences between metatorbernite and metazeunerite.

Conclusions

We have shown the presence of a complete solid solution between the end member phases metatorbernite and metazeunerite (Cu(UO₂)₂(PO₄)_{2-x}(AsO₄)_x·8H₂O) through a controlled synthetic study. Refinement of the lattice parameters confirmed all the solid solution members crystallised in a primitive tetragonal unit cell. The scatter of the *c* unit cell parameter as a function of composition, was suggested to be due to the variable water content

Phil. Trans. R. Soc. A.

1
2
3
4
5
6
7
8
9 of these samples as well as structural differences between the end member phases, whereby metatorbernite
10 crystallises in space group P4/n, but metazeunerite crystallises in space group P4/ncc. However, we found a
11 linear correlation between the a unit cell parameter and the AsO_4/PO_4 ratio (x in the solid solution
12 $\text{Cu}(\text{UO}_2)_2(\text{PO}_4)_{2-x}(\text{AsO}_4)_x \cdot 8\text{H}_2\text{O}$).
13
14
15
16

17 We have refined the lattice parameters of mineral samples of metatorbernite type phases, found to be present
18 at the South Terras site and compared to the synthetic samples to predict their compositions using the
19 relationship established between a and the AsO_4/PO_4 ratio. Our results on the natural samples obtained from
20 the South Terras site, show they may contain mixtures of arsenate and phosphate where arsenate is significant
21 and possibly dominant. While the stability of the phosphate end member, metatorbernite, in the natural
22 environment has been documented, much less is known about the arsenate material or compositions
23 containing mixtures of AsO_4 and PO_4 species, which appear to present naturally. This suggests stability
24 studies on the mixed anion materials will be of major interest in assessing the stability of the mine spoil on a
25 long term basis.
26
27
28
29
30
31
32
33

34 The stability of the two end member phases and the composition $\text{Cu}(\text{UO}_2)_2(\text{PO}_4)(\text{AsO}_4) \cdot 8\text{H}_2\text{O}$ were studied
35 using high resolution synchrotron powder diffraction data as a function of temperature. These phases have
36 been found to have different behaviour as a function of temperature. On cooling metatorbernite remains
37 primitive tetragonal and on heating above 373 K the sample becomes amorphous to X rays. The composition
38 $\text{Cu}(\text{UO}_2)_2(\text{PO}_4)(\text{AsO}_4) \cdot 8\text{H}_2\text{O}$ remains tetragonal on cooling and on heating, with a noticeable decrease in unit
39 cell parameters at 423K before transforming to a new structure type at 473K. In the case of metazeunerite, on
40 cooling the symmetry lowers and the data were indexed on a primitive orthorhombic unit cell. The sample
41 transforms to the tetragonal phase on heating above RT and on continued heating under goes a phase
42 transition likely due to water loss to a new phase which is still to be identified.
43
44
45
46
47
48
49
50

51 This preliminary study shows that natural samples of metatorbernite-type phases can have variable
52 compositions, which may effect their stability in nature. Uranium is an environmental contaminant
53 throughout the world, especially in areas where mining and milling of U were carried out, such as South
54 Terras. Uranyl phosphate phases are key in controlling U-mobility and studies have suggested using the
55
56
57

58 *Phil. Trans. R. Soc. A.*
59
60

1 R. Soc. open sci. article template

2 14 Metatorbernite-metazeunerite solid solution

3
4
5
6
7
8
9
10 precipitation of metatorbernite-type phases to decontaminate groundwater contaminated by U through
11 addition of polyphosphate. However, as we have shown, their stability is variable, dependent upon the
12 composition. Therefore, understanding any stability changes as a function of composition will be key to their
13 use as remediation materials. Ongoing studies into the structures and stabilities of phases in the
14 metatorbernite-metazeunerite solid solution is underway.
15
16
17
18
19

20 Acknowledgements

21 We would like to acknowledge Joan Sutherland and Dr Oliver Preedy for the assistance in synthesising
22 samples for data collection at the Diamond Light Source and for their assistance during the beamtime. The
23 authors would like to thank Prof Chiu Tang, Dr Sarah Day and Dr Claire Murray, beamline scientists on the
24 I11 beamline at The Diamond Light Source, for their assistance in setting up the beamline to carry out these
25 experiments.
26
27
28
29
30
31
32
33

34 Funding

35 This work was supported by the Natural Environment Council (NE/L000202/1) through a studentship for JK
36 and STFC for funding the Diamond Light Source beamtime (EE15103).
37
38
39
40
41
42

43 References

- 44
45
46 1. Kanematsu M, Perdrial N, Un W, Chorover J, O'Day P. A. 2014 Influence of phosphate and silica on U(VI)
47 precipitation from acidic and neutralised wastewaters. *Environmental Science and Technology*, **48**, 6097-6106
48
49 2. Cretaz F, Szenknect S, Clavier N. 2013 Solubility properties of synthetic and natural metatorbernite. *Journal*
50 *of Nuclear Materials*, **442**, 195-270
51
52 3. Finch R, Murakami T. 1999 Systematics and paragenesis of uranium minerals. *Uranium: mineralogy, geology*
53 *and the environment; P. C. Burns and R. Finch, Eds., Washington D. C., Mineralogical Society of America*, 91-179
54
55
56
57

58 *Phil. Trans. R. Soc. A.*
59
60

-
4. Read D, Hooker P. J, Ivanovich M, Milodowski A. E. 1991 A natural analogue study of an abandoned uranium mine in Cornwall, England. *Radiochimica Acta* **52/53**, 349-356
 5. Siddeeg S. M, Bryan N. D, Livens F. R. 2015 Behaviour and mobility of U and Ra in sediments near an abandoned uranium mine, Cornwall, UK. *Environmental Science: Processes and Impacts* **17**, 235-245
 6. Moliner-Martinez Y, Campins-Falco P, Worsfold P. J, Keith-Roach M. J. 2004 The impact of a disused mine on uranium transport in the River Fal, South West England. *Journal of Environmental Monitoring* **6**, 907-913
 7. Corkhill C. L, Crean D. E, Bailey D. J, Makepeace C, Stennett M. C, Tappero R, Grolimund D, Hyatt N. C. 2017 Multi-scale investigation of uranium attenuation by arsenic at an abandoned uranium mine, South Terras. *Materials Degeneration* **1**, 1-7
 8. Cook R. B. 1998 Metatorbernite Shaba District, Zaire *Rocks and Minerals* **73**, 352-354
 9. Smith D. K. 1984 Uranium mineralogy, *Uranium geochemistry, mineralogy, geology, exploration and resources*, London, *The Institute of Mining and Metallurgy*, 43-88
 10. Frondel C. 1958 Systematic mineralogy of uranium and thorium *United States Geological Survey Bulletin*, Washington D.C. 1064
 11. Locock A. J. 2007 Crystal chemistry of actinide phosphates and arsenates *Structural chemistry of inorganic actinide compounds*, S. V. Krivovichev, P. C. Burns and I. G. Tananaev, Eds., Amsterdam, Elsevier, 217-278
 12. Locock A. J, Burns P. C. 2003 Crystal structures and synthesis of the copper-dominant members of the autunite and meta-autunite groups: torbernite, zeunerite, metatorbernite and metazeunerite *The Canadian Mineralogist* **41**, 489-502
 13. Dowty E. ATOMS V6.1 © 2003 Shape Software
 14. Frondel J. W. 1951 Studies of uranium minerals (VII): Zeunerite *The American Mineralogist* **36**, 249-255
 15. Ross M, Evans H. T, Appleman D. E. 1964 Studies of the torbernite minerals (II): the crystal structure of meta-torbernite. *The American Mineralogist* **49**, 1603-1621
 16. Hanic F. 1960 The crystal structure of meta-zeunerite $\text{Cu}(\text{UO}_2)_2(\text{AsO}_4)_2 \cdot 8\text{H}_2\text{O}$. *Czechoslovak Journal of Physics* **10**, 169-181
 17. Donnay G, Donnay J. D. H. 1955 Contribution to the crystallography of uranium minerals, in Contribution to the Crystallography of Uranium Minerals *U.S. Geological Survey, Washington D.C.*, 1955.;
 18. Hennig C, Reck G, Reich T, Robberg A, Kraus W, Sieler J. 2003 EXAFS and XRD investigations of zeunerite and meta-zeunerite. *Zeitschrift für Kristallographie* **218**, 37-45
- Phil. Trans. R. Soc. A.*

1 R. Soc. open sci. article template

2 16 Metatorbernite-metazeunerite solid solution

3
4
5
6
7
8
9
10 19. Calos N. J, Kennard C. H. L. 1996 Crystal structure of copper bis(uranyl phosphate) octahydrate
11 (metatorbernite), $\text{Cu}(\text{UO}_2\text{PO}_4)_2 \cdot 8(\text{H}_2\text{O})$. *Zeitschrift fur Kristallographie* **211**, 701-702

12
13 20. Makarov E. S, Tobelko K. I. 1960 Crystal structure of metatorbernite. *Doklady Akademii Nauk SSSR* **131**, 87-
14 89

15
16 21. Stergiou A. C, Rentzeperis P. J. 1993 Refinement of the crystal structure of metatorbernite. *Zeitschrift für*
17 *Kristallographie* **205**, 1-7

18
19 22. Kulaszewska J. M. 2018 Stability and structure of the $\text{Cu}(\text{UO}_2)_2(\text{PO}_4)_{2-x}(\text{AsO}_4)_x \cdot 8\text{H}_2\text{O}$ solid solution and its
20 environmental significance, *PhD thesis, Loughborough University*

21
22 23. Thompson S.P, Parker J.E, Potter J, Hill T.P, Birt A, Cobb T.M, Yuan F, Tang C.C, 2009 *Review of Scientific*
23 *Instruments* **80** 075107e075109.

24
25 24. Coelho A.A. 2012 TOPAS Academic: General Profile and Structure Analysis Software for Powder
26 Diffraction Data. *Bruker AXS, Karlsruhe, Germany*

27
28 25. Walenta K. 1964 Beiträge zuer Kenntnis seltener Arsenatminerale unter besonderer Berücksichtigung von
29 Vorkommen des Schwarzwaldes. *Tschermaks mineralogische und petrographische Mitteilungen* **9**, 111-174

30
31 26. Dorhout P. K, Rosenthal G. L, Ellis A. B. 1988 Solid solutions of hydrogen uranyl phosphate and hydrogen
32 uranyl arsenate. A family of luminescent, lamellar hosts. *Inorganic Chemistry* **27**, 1159-1162

33
34 27. Dorhout P. K, Rosenthal G. L, Ellis A. B. 1989 Two families of lamellar, luminescent solid solutions: The
35 intercalative conversion of hydrogen uranyl phosphate arsenates to uranyl phosphate arsenates. *Solid State*
36 *Ionics* **32/33**, 50-56

37
38 28. Stubbs J. E, Post J. E, Elbert D. C, Heaney P. J, Veblen D. R. 2010 Uranyl phosphate sheet reconstruction
39 during dehydration of metatorbernite. *The American Mineralogist* **95**, 1132-1140

40
41 29. Suzuki Y, Sato T, Isobe H, Kogure T, Murakami T. 2005 Dehydration processes in the meta-autunite group
42 minerals meta-autunite, metasaleetite and metatorbernite. *The American Mineralogist*, **90**, 1308-1314

43
44 30. Vochten R. F. 1983 Formation of secondary uranyl phosphates in the oxidation zone of uranium deposits.
45 *Geological Society of South Africa, Johannesburg; Special publication, J. P. R. De Villiers and P. A. Cawthorn, Eds.,*
46 *Johannesburg, Geological Society of South Africa, 287-293*

47
48
49
50
51
52
53
54
55
56
57
58 *Phil. Trans. R. Soc. A.*

31. Frost R. L, Kristpf J, Weier M. L, Martens W. N, Horvath E. 2005 Thermal decomposition of metatorbernite – a controlled rate thermal decomposition. *Journal of Thermal Analysis and Calorimetry* **79**, 721-725
32. Frost R. L, Weier M. L, Adebajo M. O. 2004 Thermal decomposition of metazeunerite - a high resolution thermogravimetric and hot-stage raman spectroscopic study. *Thermochimica Acta* **419**, 119-129
33. Vochten R, Goeminne A. 1984 Synthesis, crystallographic data, solubility and electrokinetic properties of meta-zeunerite, meta-kirchheimerite and nickel-uranylarsenate. *Physics and Chemistry of Minerals* **11**, 95-100

Tables

Sample	a (Å)	c (Å)	X
HR001	7.060 (4)	17.400 (1)	1.2
Bulk HA sample	7.018 (6)	17.394 (2)	0.6

Figure and table captions

Figure 1. ac projection of the structure of metatorbernite: Red CuO_6 octahedra, green UO_6 square bipyramids and yellow PO_4 tetrahedra are shown, small and large blue spheres represent O atoms. Structure reproduced after [12] using the ATOMS V6.1 atomic structure display package [13].

Figure 2. PXRD pattern of spoil heap sub sample with high activity compared to ICDD PDF for metatorbernite, (ICDD PDF 36-406 [15]) and metazeunerite (ICDD PDF 17-146 [25]) and quartz (ICDD PDF 46-1045). Data were collected on a laboratory X ray diffractometer using $\text{Co K}\alpha_1$ radiation.

Figure 3. Comparison of unit cell parameters of the metatorbernite-metazeunerite $(\text{Cu}(\text{UO}_2)_2(\text{PO}_4)_2 \cdot x(\text{AsO}_4)_x \cdot n\text{H}_2\text{O})$ solid solution refined from laboratory PXRD data. Filled blue circles refined unit cell parameter a (bottom), filled orange triangles refined unit cell parameters c (top).

Figure 4. Refined lattice parameters from variable temperature study of metatorbernite $(\text{Cu}(\text{UO}_2)_2(\text{PO}_4)_2 \cdot 8\text{H}_2\text{O})$ and the composition $\text{Cu}(\text{UO}_2)_2(\text{PO}_4)(\text{AsO}_4) \cdot 8\text{H}_2\text{O}$ compared with reported unit cell parameters from a variable temperature study on a mineral sample of metatorbernite [27]. Grey filled circles metatorbernite a , yellow filled triangles metatorbernite c , blue filled diamonds $\text{Cu}(\text{UO}_2)_2(\text{PO}_4)(\text{AsO}_4) \cdot 8\text{H}_2\text{O}$ a , *Phil. Trans. R. Soc. A.*

1 *R. Soc. open sci.* article template

2 18 Metatorbernite-metazeunerite solid solution

3
4
5
6
7
8
9
10 green filled squares $\text{Cu}(\text{UO}_2)_2(\text{PO}_4)(\text{AsO}_4)\cdot 8\text{H}_2\text{O}$ *c*, blue open circles reported metatorbernite *a*, red open
11 triangles reported metatorbernite *c* [28]. Note, error bars on the refined parameters were smaller than the
12 markers used.
13
14

15
16
17 **Figure 5.** Refined lattice parameters from variable temperature study of metazeunerite

18 $(\text{Cu}(\text{UO}_2)_2(\text{AsO}_4)_2\cdot 8\text{H}_2\text{O})$. Blue filled circles metazeunerite *a* in tetragonal space group, red filled triangles
19 metazeunerite *c* in tetragonal space group, green filled crosses metazeunerite *a* in orthorhombic space group,
20 purple filled diamonds metazeunerite *b* in orthorhombic space group, blue filled squares metazeunerite *c* in
21 orthorhombic space group. Note, error bars on the refined parameters were smaller than the markers used.
22
23
24
25

26
27 **Table 1.** Refined unit cell parameters from two natural samples of metatorbernite-type phases and the
28 calculated *x* value from equation 1.
29
30
31
32
33
34
35
36
37
38
39
40
41
42
43
44
45
46
47
48
49
50
51
52
53
54
55
56
57

58 *Phil. Trans. R. Soc. A.*
59
60

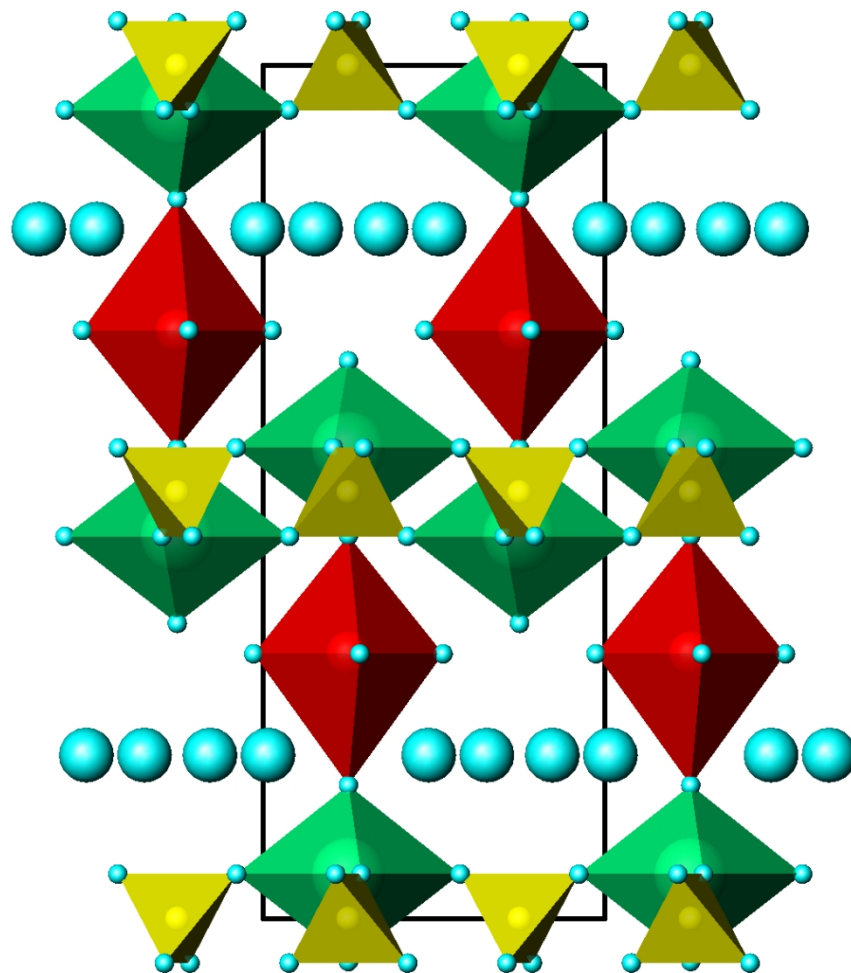


Figure 1. *ac* projection of the structure of metatorbernite: Red CuO_6 octahedra, green UO_6 square bipyramids and yellow PO_4 tetrahedra are shown, small and large blue spheres represent O atoms in the structure [12,13].

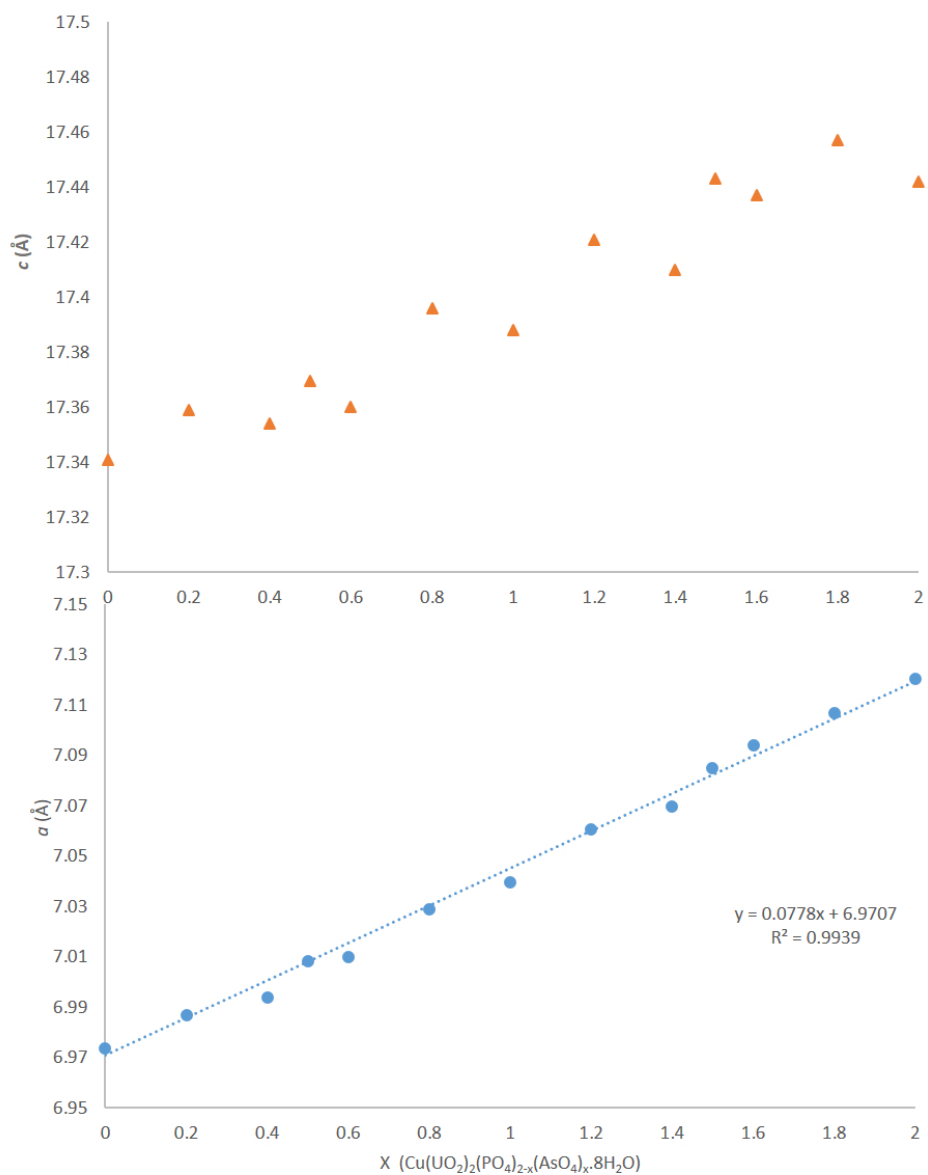


Figure 3. Comparison of unit cell parameters of the metatorbernite-metazeunerite $(\text{Cu}(\text{UO}_2)_2(\text{PO}_4)_2 \cdot x(\text{AsO}_4)_x \cdot n\text{H}_2\text{O})$ solid solution refined from laboratory PXRD data. Filled blue circles refined unit cell parameter a (bottom), filled orange triangles refined unit cell parameters c (top).

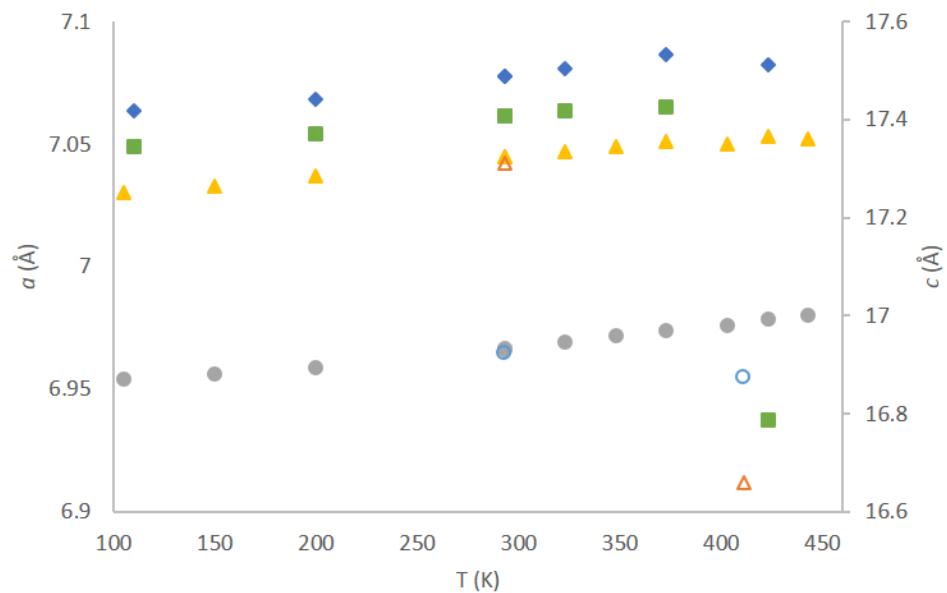


Figure 4. Refined lattice parameters from variable temperature study of metatorbernite ($\text{Cu}(\text{UO}_2)_2(\text{PO}_4)_2 \cdot 8\text{H}_2\text{O}$) and the composition $\text{Cu}(\text{UO}_2)_2(\text{PO}_4)(\text{AsO}_4) \cdot 8\text{H}_2\text{O}$ compared with reported unit cell parameters from a variable temperature study on a mineral sample of metatorbernite [28]. Grey filled circles metatorbernite a , yellow filled triangles metatorbernite c , blue filled diamonds $\text{Cu}(\text{UO}_2)_2(\text{PO}_4)(\text{AsO}_4) \cdot 8\text{H}_2\text{O}$ a , green filled squares $\text{Cu}(\text{UO}_2)_2(\text{PO}_4)(\text{AsO}_4) \cdot 8\text{H}_2\text{O}$ c , blue open circles reported metatorbernite a , red open triangles reported metatorbernite c [29]. Note, error bars on the refined parameters were smaller than the markers used.

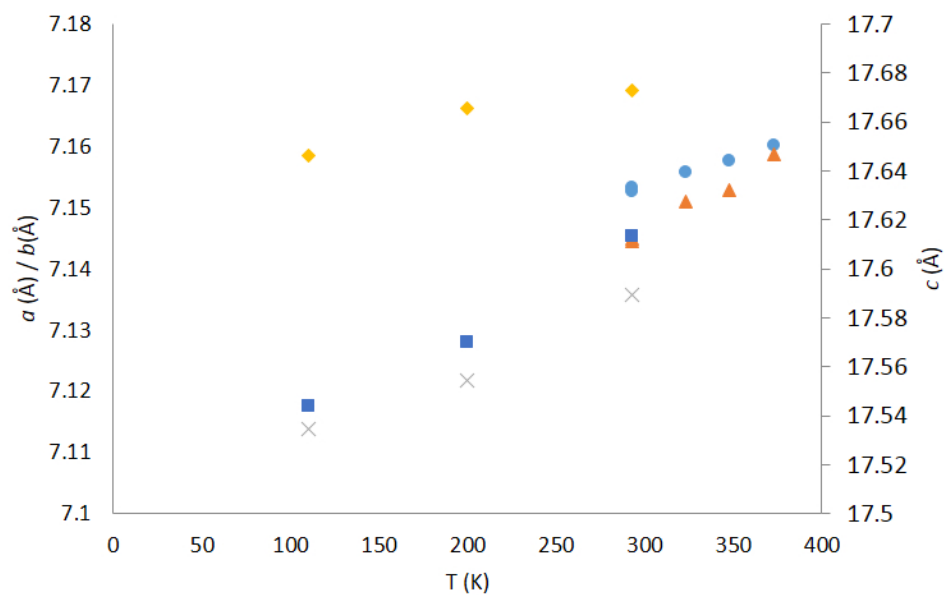


Figure 5. Refined lattice parameters from variable temperature study of metazeunerite ($\text{Cu}(\text{UO}_2)_2(\text{AsO}_4)_2 \cdot 8\text{H}_2\text{O}$). Blue filled circles metazeunerite a in tetragonal space group, red filled triangles metazeunerite c in tetragonal space group, green filled crosses metazeunerite a in orthorhombic space group, yellow filled diamonds metazeunerite b in orthorhombic space group, blue filled squares metazeunerite c in orthorhombic space group. Note, error bars on the refined parameters were smaller than the markers used.